Clinical Microbiology and Infection 28 (2022) 1367–1374

Contents lists available at ScienceDirect

Clinical Microbiology and Infection

journal homepage: www.clinicalmicrobiologyandinfection.com

Original article

Translational *in vitro* and *in vivo* PKPD modelling for apramycin against Gram-negative lung pathogens to facilitate prediction of human efficacious dose in pneumonia

Vincent Aranzana-Climent [1], Diarmaid Hughes [2], Sha Cao [2], Magdalena Tomczak [3], Malgorzata Urbas [3], Dorota Zabicka [3], Carina Vingsbo Lundberg [4], Jon Hansen [4], Johan Lindberg [5], Sven N. Hobbie [6], Lena E. Friberg [1, *]

[1] *Department of Pharmacy, Uppsala University, Uppsala, Sweden*
[2] *Department of Medical Biochemistry and Microbiology, Uppsala University, Uppsala, Sweden*
[3] *Department of Epidemiology and Clinical Microbiology, National Medicines Institute, Warsaw, Poland*
[4] *Bacteria, Parasites & Fungi, Statens Serum Institut, Copenhagen, Denmark*
[5] *RISE Research Institutes of Sweden, Södertalje, Sweden*
[6] *Institute of Medical Microbiology, University of Zurich, Zurich, Switzerland*

ARTICLE INFO

Article history:
Received 18 December 2021
Received in revised form
23 April 2022
Accepted 3 May 2022
Available online 20 May 2022

Editor: E. Yusuf

Keywords:
Apramycin
Modelling
Pharmacodynamics
Pharmacokinetics
Pharmacometrics
Preclinical
Translational

ABSTRACT

Objectives: New drugs and methods to efficiently fight carbapenem-resistant gram-negative pathogens are sorely needed. In this study, we characterized the preclinical pharmacokinetics (PK) and pharmacodynamics of the clinical stage drug candidate apramycin in time kill and mouse lung infection models. Based on *in vitro* and *in vivo* data, we developed a mathematical model to predict human efficacy.
Methods: Three pneumonia-inducing gram-negative species *Acinetobacter baumannii*, *Pseudomonas aeruginosa*, and *Klebsiella pneumoniae* were studied. Bactericidal kinetics were evaluated with time-kill curves; *in vivo* PK were studied in healthy and infected mice, with sampling in plasma and epithelial lining fluid after subcutaneous administration; *in vivo* efficacy was measured in a neutropenic mouse pneumonia model. A pharmacokinetic-pharmacodynamic model, integrating all the data, was developed and simulations were performed.
Results: Good lung penetration of apramycin in epithelial lining fluid (ELF) was shown (area under the curve $(AUC)_{ELF}/AUC_{plasma}$ = 88%). Plasma clearance was 48% lower in lung infected mice compared to healthy mice. For two out of five strains studied, a delay in growth (~5 h) was observed *in vivo* but not *in vitro*. The mathematical model enabled integration of lung PK to drive mouse PK and pharmacodynamics. Simulations predicted that 30 mg/kg of apramycin once daily would result in bacteriostasis in patients.
Discussion: Apramycin is a candidate for treatment of carbapenem-resistant gram-negative pneumonia as demonstrated in an integrated modeling framework for three bacterial species. We show that mathematical modelling is a useful tool for simultaneous inclusion of multiple data sources, notably plasma and lung *in vivo* PK and simulation of expected scenarios in a clinical setting, notably lung infections. **Vincent Aranzana-Climent, Clin Microbiol Infect 2022;28:1367**
© 2022 The Author(s). Published by Elsevier Ltd on behalf of European Society of Clinical Microbiology and Infectious Diseases. This is an open access article under the CC BY license (http://creativecommons.org/licenses/by/4.0/).

Introduction

Carbapenem-resistant gram-negative lung pathogens, such as *Acinetobacter baumannii*, *Pseudomonas aeruginosa,* and *Klebsiella pneumoniae* are listed as critical priority pathogens by both the WHO and the CDC [1,2]. To combat these infections, new drugs are currently in development, among which EBL-1003, a crystalline

* Corresponding author: Lena Friberg, Uppsala University, Department of Pharmacy, Box 580, 75123 Uppsala, Sweden.
E-mail address: lena.friberg@farmaci.uu.se (L.E. Friberg).

https://doi.org/10.1016/j.cmi.2022.05.003
1198-743X/© 2022 The Author(s). Published by Elsevier Ltd on behalf of European Society of Clinical Microbiology and Infectious Diseases. This is an open access article under the CC BY license (http://creativecommons.org/licenses/by/4.0/).

free base of apramycin, is a candidate drug currently in clinical development [3,4]. Apramycin has a distinctive chemical structure among aminoglycosides that makes it evade all resistance mechanisms of clinical relevance, including aminoglycoside-modifying enzymes such as acetyltransferases, phosphotransferases, and nucleotidyltransferases, but also 16S-ribosomal RNA methyltransferases such as ArmA, RmtB, RmtC, and related isoforms [5]. *In vitro* [5–15] and *in vivo* [16–19] activity of apramycin against multiple bacterial species including *Escherichia coli* and *A. baumannii* strains has been previously shown. Expanding on promising activity seen against one pneumonia-inducing *A. baumannii* strain [17], the present study extends our knowledge of apramycin *in vitro* and *in vivo* lung infection activity to two new gram-negative pneumonia-inducing species. Mathematical pharmacokinetic-pharmacodynamic (PKPD) modelling of preclinical data is increasingly used for translation of preclinical results during drug development [20,21] and was applied to apramycin *in vitro* and mouse thigh infection data against *E. coli* [16]. The current study goes one step further, by including epithelial lining fluid concentrations (ELF) to drive the *in vivo* effect and make predictions of expected effect in humans with pneumonia.

Methods

Strains

Five clinical isolates were studied (see Supplementary material, Table S1)—two *A. baumannii* strains AR Bank #0282 (apramycin MIC = 4 mg/L) and AR Bank #0277 (MIC = 16 mg/L), two *K. pneumoniae* 3010 and ST258 (MIC = 1 mg/L for both), and one *P. aeruginosa* AMA1385 (MIC = 8 mg/L).

In vitro time-kill curves

The bactericidal activity of apramycin was assessed in time-kill experiments. In brief, an overnight culture was diluted 100-fold in pre-warmed Mueller Hinton II (MHII) broth, grown 1.5 hours to logarithmic phase (OD_{600} 0.1–0.3), and used to inoculate tubes containing 2 mL of pre-warmed Mueller Hinton II medium to attain ~10^6 colony forming units (CFU). Apramycin was added to the tubes to achieve concentrations ranging from 0.25 to 16 × MIC. The tubes were incubated at 37°C with shaking at 150 rpm. Samples were drawn for viable counts at 0, 1, 2, 4, 6, 8, 24, and 28 hours. After incubation at 37°C for 18 to 24 hours on agar plates, CFU was counted manually. The limit of detection was 1 CFU/mL. Four experiments were performed for *K. pneumoniae* 3010 and one experiment for the other strains.

PD modelling based on in vitro data

The *in vitro* time-kill data was analysed using semi-mechanistic PKPD modelling. Details are presented in the Supplementary material (Text S1).

Mouse lung infection model

PK and PKPD studies with a murine lung infection model were conducted at Pharmacology Discovery Services Taiwan Ltd. and Statens Serum Institute (Copenhagen, Denmark) in full compliance with the International Guiding Principles for Biomedical Research and approval by local animal ethics committees. Mice were immunosuppressed by intraperitoneal injections of cyclophosphamide and intranasally infected with a target inoculum of 1×10^6 CFU/mouse.

Mouse PK experiments and modelling

Apramycin PK was studied in neutropenic infected and non-infected mice (see Supplementary material, Table S2). Briefly, apramycin doses ranging from 20 to 400 mg/kg were tested across multiple experiments. Apramycin was injected 2 hours post infection. Plasma and bronchoalveolar lavage fluid samples were collected at times ranging from 10 minutes to 42 hours post first dose. Drug and urea concentrations in plasma and bronchoalveolar lavage were quantified by LC-MS/MS as described previously [16]. Drug concentrations in ELF were normalized for urea content:

$$[Drug\ Concentration]_{ELF} = [Drug\ Concentration]_{BAL} \times \left(\frac{[Urea\ concentration]_{plasma}}{[Urea\ concentration]_{BAL}}\right) \quad (1)$$

An unbound fraction of apramycin in mouse plasma of 91.6% was used (in-house data). Models with 4- and 5-compartments simultaneously describing plasma and ELF PK were tested (see Supplementary material, Fig. S1). The model building procedure is detailed in the Supplementary material (Text S2).

Mouse PKPD experiments and PKPD modelling

The same five strains were studied *in vivo* as *in vitro*. Subcutaneous treatment with apramycin started 2 hours post infection. Doses ranged from 0.55 to 400 mg/kg with dosing intervals ranging from every 2 hours to every 24 hours (see Supplementary material, Table S3). Mice were euthanized 26 hours post infection for the treated groups, and 2, 4, 6, 8, 12, and 18 hours post infection for the control mice. Both lungs were harvested, homogenized in sterile 0.9% NaCl then CFU per two lungs (CFU/total lung) were determined after 18 to24 hours incubation at 35°C. The best fitting PKPD-model based on *in vitro* time-kill data and the best fitting PK model were combined to form the structural model for *in vivo* mouse PKPD data. Then, PD parameters were re-estimated using *in vivo* data (see Supplementary material, Text S3).

Prediction of human efficacy

The PK of apramycin is similar to that of gentamicin, as shown in three different animal species (in-house data) [16]. Plasma and ELF concentration-time courses in adult hospitalised patients were simulated from a PK model of gentamicin [22], selected because it includes distribution to ELF. An unbound fraction of 92.9% in human plasma (in-house data) was applied.

The human PK model was combined with the PD component of the mouse PKPD model to predict bacterial burden over 24 hours in

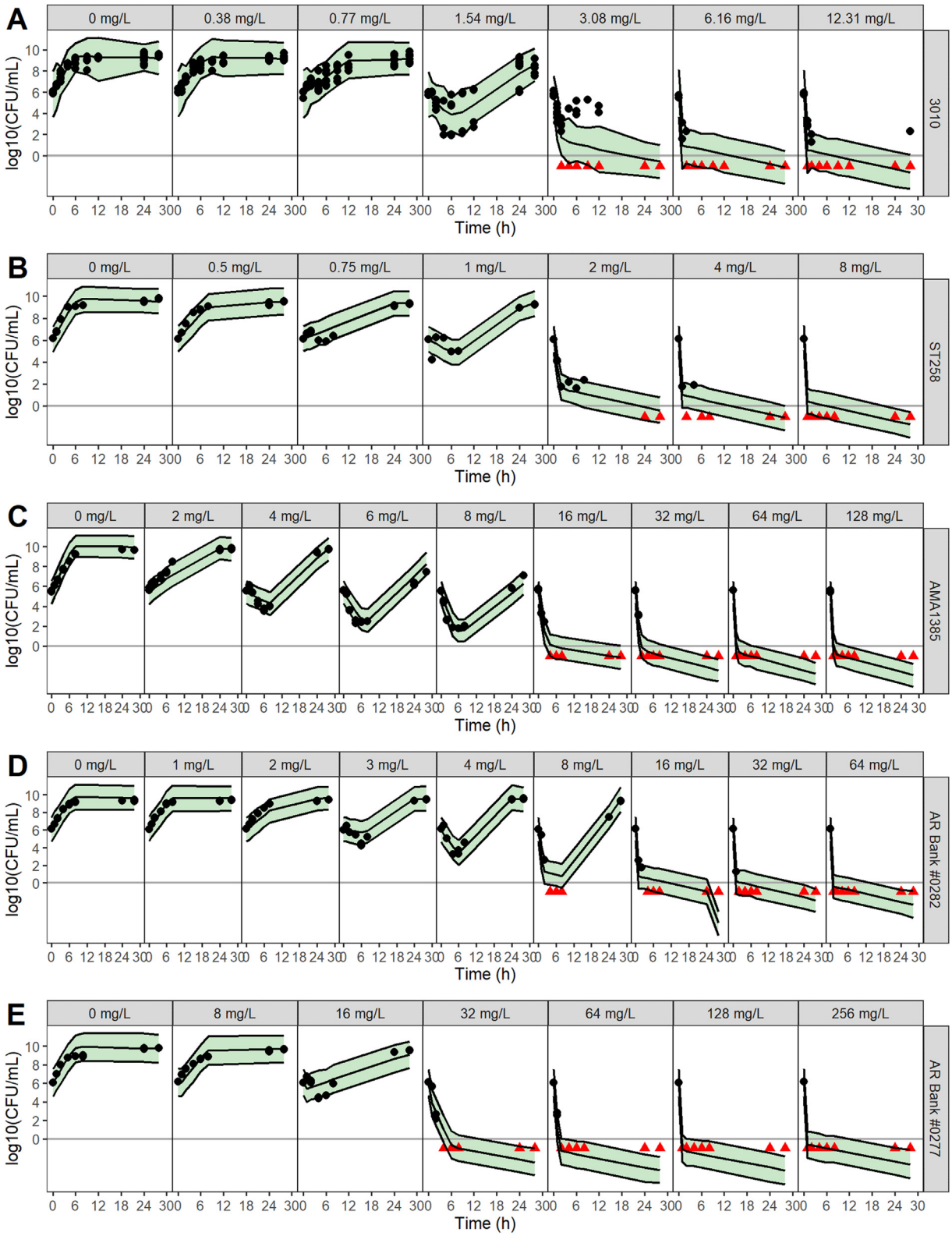

Fig. 1. Visual predictive checks of the final model based on *in vitro* time-kill data. The plots show the observed time-kill data at different apramycin concentrations with model predictions as medians and 95% CIs around the median (shaded area). Dots represent countable plates; triangles represent data below the limit of quantification (BLQ: 1 log10 colony forming units (CFU)/mL). Data below the limit of detection are plotted as 0.1 CFU/mL. (a) *Klebsiella pneumoniae* 3010, (b) *K. pneumoniae* ST258, (c) *Pseudomonas aeruginosa* AMA1385, (d) *Acinetobacter baumannii* AR Bank #0282, and (e) *A. baumannii* AR Bank #0277.

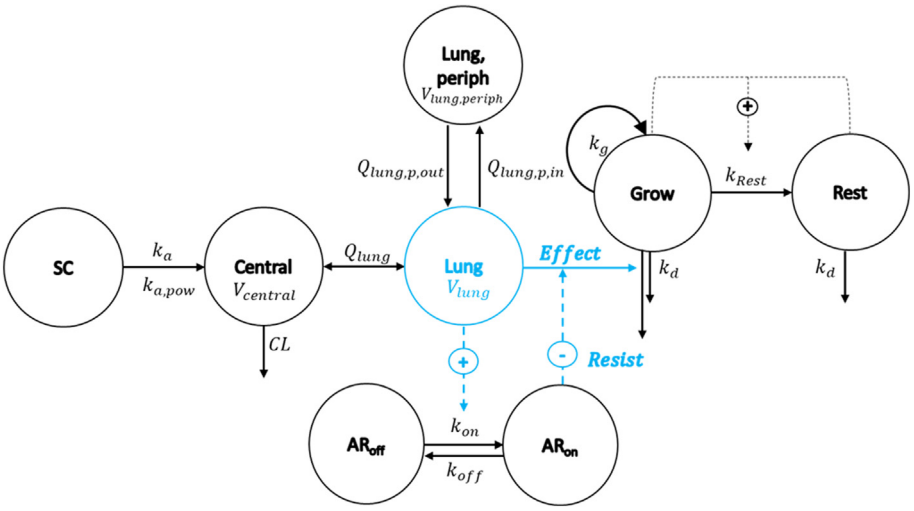

Fig. 2. Schematic representation of the final *in vivo* PKPD model. Grow: Growing bacterial subpopulation. Parameters are defined in Supplementary material (Table S4) and model equations. Abbreviations: Rest: resting bacterial subpopulation; AR_{on}/AR_{off}, virtual compartments representing the fraction of adapted and non-adapted bacteria, respectively.

humans. Predictions were performed for single doses of 10, 20, 30, and 40 mg/kg administered over 30 min, in a 70 kg adult with reduced creatinine clearance (CrCL = 80 mL/min) and a 70 kg adult with a 'normal' CrCl (120 mL/min). Initial bacterial densities of 10^6 and $10^{7.5}$ CFU/total lung were explored.

Model building and evaluation

Model selection was based on the difference in objective function value (dOFV) where a difference of at least 10.83 was required to select a model with one additional parameter, as well as graphical evaluations [23]. NONMEM v7.5.0 (Icon PLC, Dublin, Ireland) was used for model fitting and to perform SIR [24] and VPCs [25]. R [26] was used for data management and graphics.

Results

In vitro time kill curves and PD modelling

For all five strains, bacterial killing was followed by regrowth for at least one tested concentration of apramycin (Fig. 1). The final model for all strains included adaptive resistance (Fig. 2, see Supplementary material, Equations S1–7). Under these experimental conditions (no washout) the rate constant for reversal of adaptive resistance (k_{off}) could not be estimated and was fixed to 0.005 h^{-1}, and the hill factor on the effect of adaptation on E_{max} ($Hill_{AR}$) was fixed to the upper limit of 20 (see Supplementary material, Table S4). Killing and regrowth was well described for all strains with the exception of the early regrowth for 3.08 mg/L and *K. pneumoniae* 3010 (Fig. 1).

Mouse PK experiments and modelling

A long retention of apramycin in ELF, with detectable concentrations 24 hours post dose, was observed in healthy and infected mice for doses ≥100 mg/kg. No accumulation was observed with 140 mg/kg every 6 hours (Fig. 3). The best fitting model was a 3-compartment disposition model with one compartment describing the distribution of apramycin and 2 compartments representing lung distribution, as well as 1 compartment for absorption from subcutaneous administration (Fig. 2, also see Supplementary material, Equations S8–14, Table S4). Infection had a significant effect (dOFV = 173; $p < 0.001$) on plasma CL with a 48% reduction observed in infected mice vs. non-infected mice. The final model fitted both the healthy and infected animal data well (see Supplementary material, Fig. S2). The observed area under the curve $(AUC)_{ELF}/AUC_{Plasma}$ average penetration ratio was 88% as reported earlier [17].

Mouse PKPD experiments and PKPD modelling

A delay in growth was observed for strains *A. baumannii* #0277 and *P. aeruginosa* AMA1385 (Fig. 4a). The bacterial burden was at the start of treatment 3.5×10^5, 8.1×10^5, 2.9×10^7, 2.9×10^6 and 2.5×10^5 CFU/total lung for *A. baumannii* #0277, *A. baumannii* #0282, *K. pneumoniae* 3010, *K. pneumonia* ST258, and *P. aeruginosa* AMA1385, respectively. Reduction of lung bacterial burden at 24 hours post-dose of at least 2 logs (CFU/total lung) was observed for all strains with total daily doses ≥100 mg/kg (Fig. 4b). A schematic representation of the final *in vivo* PKPD model can be found in Fig. 2 and its parameters in the Supplementary material (Table S4). Graphical evaluation showed that the model resulted in a good fit to the data (see Supplementary material, Fig. S3). For all strains, the maximum growth rate constant was lower *in vivo* than *in vitro* (range, -24% to -78%).

Prediction of human efficacy

The predicted bacterial burden in human lung after 10–40 mg/kg single doses of apramycin are presented in Fig. 5. A dose of 30 mg/kg was sufficient to yield stasis for all strains, although regrowth was predicted for *A. baumannii* #0277 and *P. aeruginosa* AMA1385, but not for *A. baumannii* #0282 and the two *K. pneumoniae* strains. Similar results were found for all strains but ST258 when using an initial bacterial density of $10^{7.5}$ CFU/total lung (see Supplementary material, Fig. S5). ST258 was predicted to require a dose of 40 mg/kg to achieve a static effect at 24 hours.

Discussion

In this study we demonstrated how *in vitro* and *in vivo* PK and PKPD data can be integrated in a comprehensive mathematical model. This technique provides a valuable alternative to the standard approach that does not negate the time-longitudinal

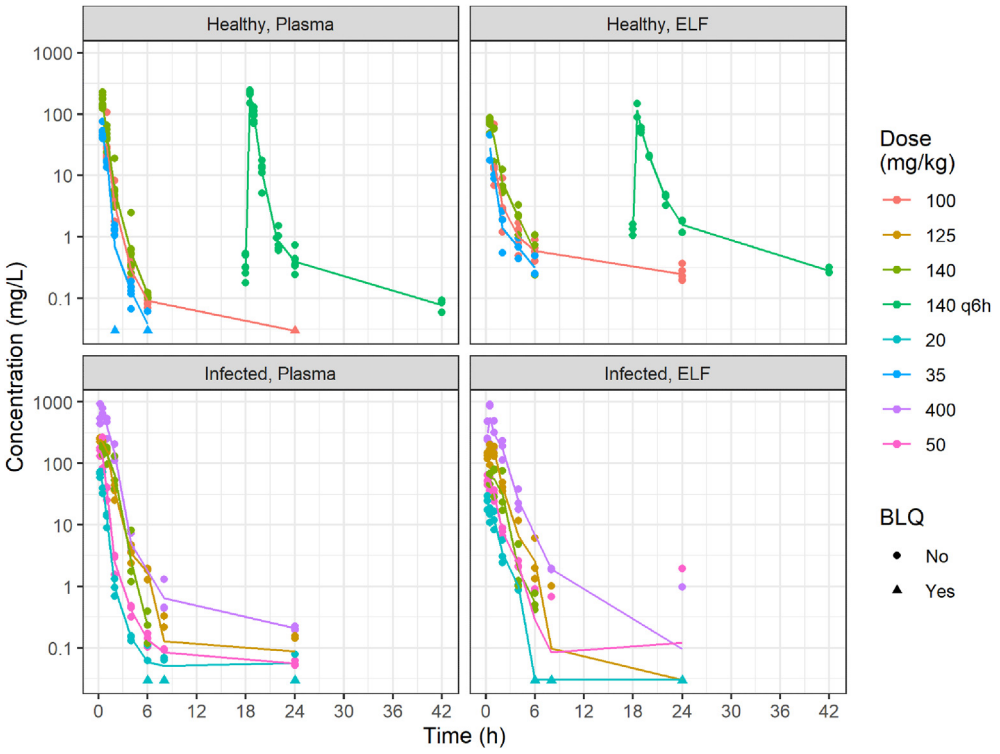

Fig. 3. *In vivo* PK data. Plasma (left) and ELF (right) PK data for healthy (top) and infected (bottom) mice. Different colours represent different dosing regimens of apramycin (single dose, except for 140 mg/kg every 6 hours). Circles are data above the limit of quantification, triangles are for data below the limit of quantification. Abbreviations: BLQ, below the limit of quantification; ELF, epithelial lining fluid; PK, pharmacokinetics.

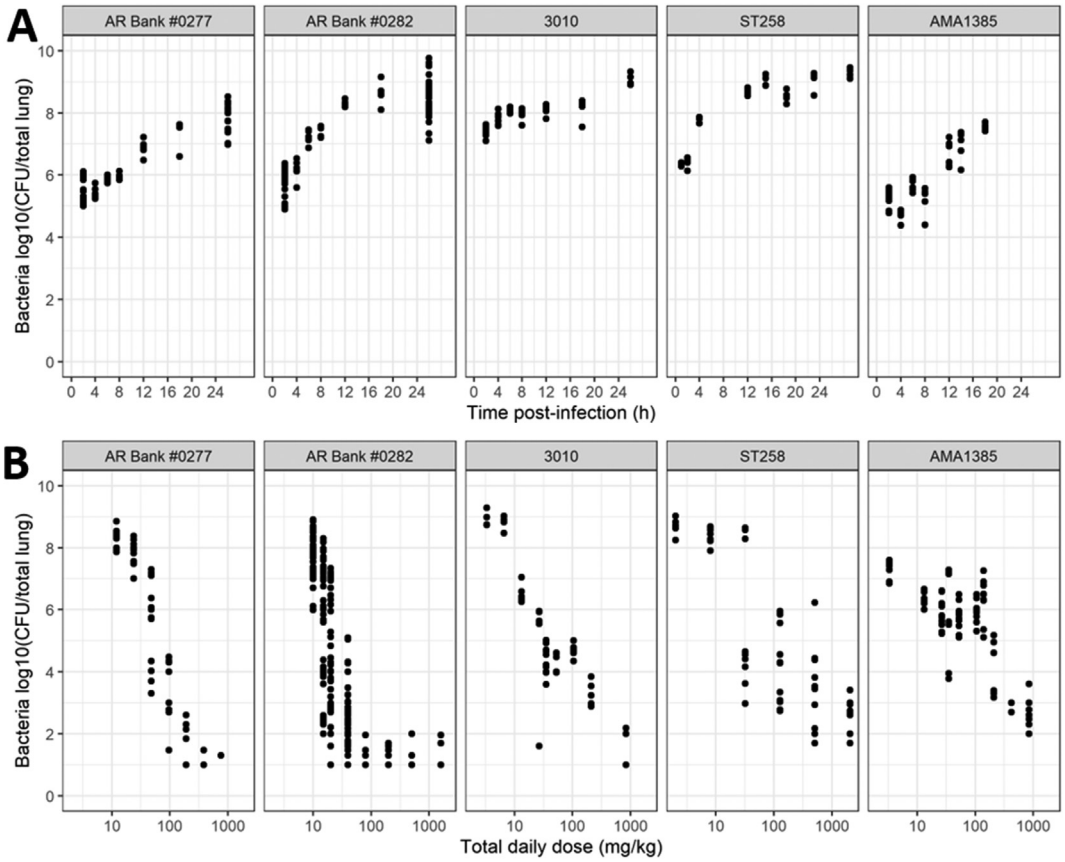

Fig. 4. *In vivo* PD data. (a) Data from infected untreated mice. (b) Data from mice treated with apramycin. Dots represent bacterial loads in individual lungs harvested 26 hours post infection. Abbreviations: CFU, colony forming unit; PD, pharmacodynamics.

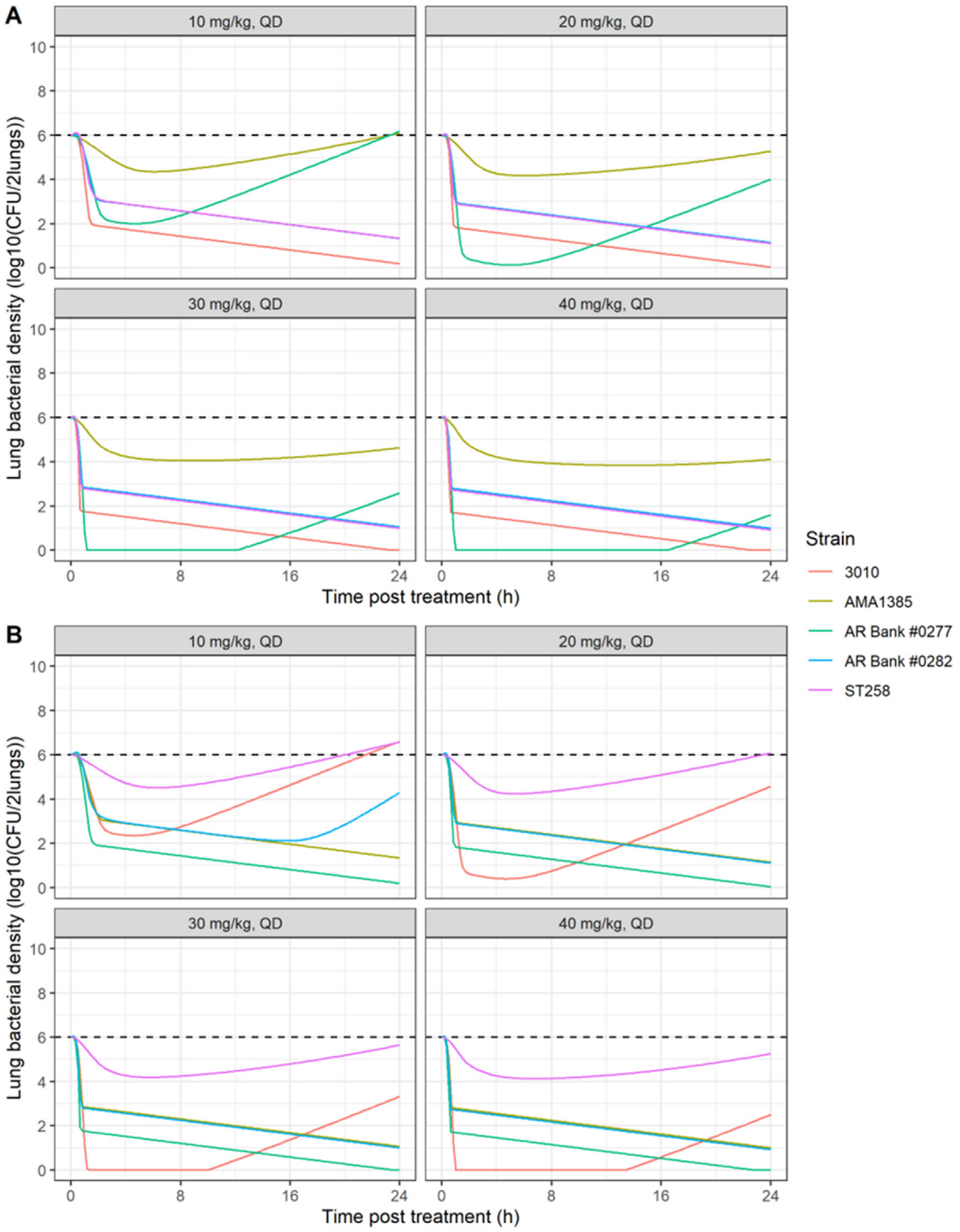

Fig. 5. Predicted efficacy in humans. Expected bacterial densities after a 30 minute infusion of apramycin at a single dose of 10, 20, 30, or 40 mg/kg apramycin. Colors represent different bacterial strains. Human pharmacokinetic profiles of the drugs were predicted for a 75 kg patient with (a) CrCL = 80 mL/min and (b) CrCL = 120 mL/min. Abbreviations: CFU, colony forming unit; CrCL, creatinine clearance; QD, every day.

component of the data contrary to the PK/PD index methodology that is only suited for single time-point data. For example, an adaptive resistance equation could characterize the observed regrowth over time, a hypothesis which is compatible with previous reports on adaptive resistance for aminoglycosides [27,28].

We showed that apramycin is a promising aminoglycoside to treat lung infection caused by gram-negative pathogens since a 30 mg/kg dose is predicted to yield at least stasis against strains with an MIC ≤8 mg/L. The range of simulated daily doses (10–40 mg/kg) was based on previous results obtained by Sou et al. [16], where they found that 30 mg/kg once daily resulted in a probability of target attainment >90% against *E. coli* isolates with MICs ≤8 mg/L.

The current study complements and advances two published studies on apramycin *in vitro* and *in vivo* evaluation. First, it expands the previous study by Sou et al. [16], where similar mathematical modelling methodology was applied to the study of apramycin against *E. coli* strains in thigh infection models. In the present study, the methodology was extended to include lung exposure and pneumonia infection. Pneumonia-relevant bacteria species were consequently studied, and the PK model was expanded to consider

both plasma and ELF concentrations and both healthy and infected animals. Secondly, PKPD-relationships for *A. baumannii* were here expanded from the traditional PK/PD-indices reported by Becker et al. [17] to predict the 24 hour time-course of bacterial growth and killing. In both Sou et al. and Becker et al. a 30 mg/kg daily dose was suggested as a promising dosing regimen for urinary tract infections (UTI) and pneumonia, respectively, to be tested in humans, which the present findings corroborate. In both studies, the suggested PK/PD index to be predictive of bacterial load reduction was AUC/MIC, which is in line with the most recent USCAST [29] and EUCAST [30] guidelines on aminoglycosides. The probability of target attainment for the 30 mg/kg once daily regimen was above 90% for both *A. baumannii* [17] and *K. pneumoniae* (in house data) strains with MICs $\leq$8 mg/L.

The principal strength of the present study lies in the integration of all data (i.e., *in vitro* PD data, *in vivo* PK, and PKPD data) within a single mathematical model that enable simultaneous consideration of all factors influencing drug effect for each of the five studied strains. Also, of interest is the originality of available data, firstly the availability of longitudinal *in vivo* control data. Traditionally, only one time-point is available from *in vivo* data. If this had been the case in the present study, the growth delay observed for some of the strains would have been missed and *in vivo* PD parameters would have been biased. Equally valuable was the availability of ELF concentrations measured in mice. This enabled correlation of the observed effect with those concentrations instead of plasma concentrations. While there is some debate about whether ELF concentrations can be considered as site-of-action concentrations for gram-negative lung infections, these concentrations are most probably closer to site of action than plasma concentrations. Thus, we think that gathering ELF data should be standard for preclinical evaluation of antibiotic efficacy in pneumonia models. Of interest was also the availability of PK data in healthy and infected mice, which enabled evaluation of an effect of infection on the PK parameters. We observed a reduced clearance of apramycin in infected animals. While it was beyond the scope of this study to find the cause; it is in line with previous results by Torres et al. [31], where reduced ciprofloxacin clearance was shown in infected animals.

One weakness of the present study was that the *in vivo* PD data of mice treated by apramycin was single time point, which only made it possible to re-estimate PD parameters but not to evaluate different model equations. In future studies, it would be valuable to gather multiple time points for treated mice to see if model differences between *in vitro* and *in vivo* data can be observed like they were observed for the control data. As part of the development plan for apramycin, it was decided to use available resources to perform apramycin time-kill curves on a wide range of strains as opposed to fewer strains with multiple replicates. The four replicates of the *K. pneumoniae* 3010 time-kill experiments provided us an estimate of expected experiment-to-experiment variability.

The present study shows that integration of *in vitro* and *in vivo* PKPD data, as well as a PK model accounting for distribution into lung, in a common model can be used to make predictions of expected effects in patients, thus increasing the value of preclinical data. This makes the approach especially valuable in drug development, allowing for various scenarios to be explored, and any new data can be used to update the model. For example, once data on apramycin distribution to the lung is available, the model predictions could be updated with new data. Since this type of approach considers the time-course and development of resistance, and allows for prediction of combination therapies, it may be more valuable than the traditional PK/PD indices.

To conclude, apramycin demonstrated good lung penetration and sustained exposure in healthy and lung-infected mice. Pharmacometric PKPD modelling facilitating the integration and interpretation of collected *in vitro* and *in vivo* data and showed that apramycin is expected to be efficacious at 30 mg/kg once daily against gram-negative lung infections in humans. A first-in-human study has been concluded (ClinicalTrials.gov ID: NCT04105205) and a human pulmonary exposure study is currently in preparation, which will further our efforts towards apramycin clinical development for use against pneumonia caused by gram-negative infection.

Transparency declaration

Some of the research leading to these results was conducted as part of the ND4BB European Gram-Negative Antibacterial Engine (ENABLE) Consortium (www.nd4bb-enable.eu) and has received funding from the Innovative Medicines Initiative Joint Undertaking (www.imi.europa.eu) under grant agreement no. 115583, resources of which are composed of financial contribution from the European Union's Seventh Framework Programme (FP7/2007-2013) and The European Federation of Pharmaceutical Industries and Associations (EFPIA) companies in-kind contribution. The ENABLE project is also financially supported by contributions from academic and small and medium-sized enterprise (SME) partners. This work was in part financially supported by the ENABLE supplementary grant W187/IMI/2014 from the Polish Ministry of Science and Higher Education. The University of Zurich has utilized the suite of preclinical services for in-vivo assessment offered by the National Institute of Allergy and Infectious Diseases (NIAID) at the National Institutes of Health (NIH) (Contract Nos. HHSN272201700020I 75N93020F00159 and HHSN272201700020I 75N93019F00131, with Pharmacology Discovery Services Taiwan, a Eurofins Discovery Partner Lab). VAC was also supported by the Swedish Research Council [grant no. 2018-03296 to LF]. SNH is a Co-Founder of Juvabis AG, which develops apramycin for human use. The other authors have no conflict of interest to declare in addition to the funding for the study detailed above. These results have been partially presented at the 31st European Congress of Clinical Microbiology and Infectious Diseases (ECCMID).

Author contributions

Conceptualization: VAC, DH, MT, CVL, JL, SNH, LF; methodology: VAC, DH, MT, CVL, JL, SNH, LF; formal analysis: VAC, LF; investigation: all authors; writing – original draft: VAC, SNH, LF; writing – review and editing: all authors; supervision: LF, SNH.

Appendix A. Supplementary data

Supplementary data to this article can be found online at https://doi.org/10.1016/j.cmi.2022.05.003.

References

[1] Tacconelli E, Carrara E, Savoldi A, Harbarth S, Mendelson M, Monnet DL, et al. Discovery, research, and development of new antibiotics: the WHO priority list of antibiotic-resistant bacteria and tuberculosis. Lancet Infect Dis 2018;18:318–27.
[2] Centers for Disease Control and Prevention (U.S.). Antibiotic resistance threats in the United States. Available at: https://stacks.cdc.gov/view/cdc/82532. [Accessed 8 November 2021].
[3] Theuretzbacher U, Bush K, Harbarth S, Paul M, Rex JH, Tacconelli E, et al. Critical analysis of antibacterial agents in clinical development. Nat Rev Microbiol 2020;18:286–98. https://doi.org/10.1038/s41579-020-0340-0.
[4] Olliver M, Griestop L, Hughes D, Belfrage AK, Gising J, Baranczewski P, et al. ENABLE: an engine for European antibacterial drug discovery and development. Nat Rev Drug Discov 2021;20:407–8. https://doi.org/10.1038/d41573-021-00074-y.
[5] Juhas M, Widlake E, Teo J, Huseby DL, Tyrrell JM, Polikanov YS, et al. In vitro activity of apramycin against multidrug-, carbapenem- and aminoglycoside-

resistant Enterobacteriaceae and Acinetobacter baumannii. J Antimicrob Chemother 2019;74:944–52. https://doi.org/10.1093/jac/dky546.
[6] Kang AD, Smith KP, Eliopoulos GM, Berg AH, McCoy C, Kirby JE. In vitro apramycin activity against multidrug-resistant Acinetobacter baumannii and Pseudomonas aeruginosa. Diagn Microbiol Infect Dis 2017;88:188–91. https://doi.org/10.1016/j.diagmicrobio.2017.03.006.
[7] Nafplioti K, Galani I, Angelidis E, Adamou P, Moraitou E, Giannopoulou P, et al. Dissemination of international clone II Acinetobacter baumannii strains coproducing OXA-23 carbapenemase and 16S rRNA methylase ArmA in Athens, Greece. Microb Drug Resist 2020;26:9–13. https://doi.org/10.1089/mdr.2019.0075.
[8] Livermore DM, Mushtaq S, Warner M, Zhang JC, Maharjan S, Doumith M, et al. Activity of aminoglycosides, including ACHN-490, against carbapenem-resistant Enterobacteriaceae isolates. J Antimicrob Chemother 2011;66:48–53. https://doi.org/10.1093/jac/dkq408.
[9] Gysin M, Acevedo CT, Haldimann K, Bodendoerfer E, Imkamp F, Bulut K, et al. Antimicrobial susceptibility patterns of respiratory Gram-negative bacterial isolates from COVID-19 patients in Switzerland. Ann Clin Microbiol Antimicrob 2021;20:64. https://doi.org/10.1186/s12941-021-00468-1.
[10] Holbrook SYL, Garneau-Tsodikova S. Evaluation of aminoglycoside and carbapenem resistance in a collection of drug-resistant Pseudomonas aeruginosa clinical isolates. Microb Drug Resist 2018;24:1020–30. https://doi.org/10.1089/mdr.2017.0101.
[11] Smith KP, Kirby JE. Evaluation of apramycin activity against carbapenem-resistant and -susceptible strains of Enterobacteriaceae. Diagn Microbiol Infect Dis 2016;86:439–41. https://doi.org/10.1016/j.diagmicrobio.2016.09.002.
[12] Hao M, Shi X, Lv J, Niu S, Cheng S, Du H, et al. In vitro activity of apramycin against carbapenem-resistant and hypervirulent Klebsiella pneumoniae isolates. Front Microbiol 2020;11:425. https://doi.org/10.3389/fmicb.2020.00425.
[13] Hu Y, Liu L, Zhang X, Feng Y, Zong Z. In vitro activity of neomycin, streptomycin, paromomycin and apramycin against carbapenem-resistant Enterobacteriaceae clinical strains. Front Microbiol 2017;8:2275. https://doi.org/10.3389/fmicb.2017.02275.
[14] Brennan-Krohn T, Kirby JE. Synergistic combinations and repurposed antibiotics active against the pandrug-resistant Klebsiella pneumoniae Nevada strain. Antimicrob Agents Chemother 2019;63. https://doi.org/10.1128/AAC.01374-19. e01374-19.
[15] Roch M, Sierra R, Sands K, Martins WMBS, Schrenzel J, Walsh TR, et al. Vertical and horizontal dissemination of an IncC plasmid harbouring rmtB 16S rRNA methylase gene, conferring resistance to plazomicin, among invasive ST258 and ST16 KPC-producing Klebsiella pneumoniae. J Glob Antimicrob Resist 2021;24:183–9. https://doi.org/10.1016/j.jgar.2020.12.006.
[16] Sou T, Hansen J, Liepinsh E, Backlund M, Ercan O, Grinberga S, et al. Model-informed drug development for antimicrobials: translational PK and PKPD modelling to predict an efficacious human dose for apramycin. Clin Pharmacol Ther 2021;109:1063–73. https://doi.org/10.1002/cpt.2104.
[17] Becker K, Aranzana-Climent V, Cao S, Nilsson A, Shariatgorji R, Haldimann K, et al. Efficacy of EBL-1003 (apramycin) against Acinetobacter baumannii lung infections in mice. Clin Microbiol Infect 2021;27:1315–21. https://doi.org/10.1016/j.cmi.2020.12.004.
[18] Becker K, Cao S, Nilsson A, Erlandsson M, Hotop SK, Kuka J, et al. Antibacterial activity of apramycin at acidic pH warrants wide therapeutic window in the treatment of complicated urinary tract infections and acute pyelonephritis. EBioMedicine 2021;73:103652. https://doi.org/10.1016/j.ebiom.2021.103652.
[19] Kang AD, Smith KP, Berg AH, Truelson KA, Eliopoulos GM, McCoy C, et al. Efficacy of apramycin against multidrug-resistant Acinetobacter baumannii in the murine neutropenic thigh model. Antimicrob Agents Chemother 2018;62. https://doi.org/10.1128/AAC.02585-17. e02585-17.
[20] Friberg LE. Pivotal role of translation in anti-infective development. Clin Pharmacol Ther 2021;109:856–66. https://doi.org/10.1002/cpt.2182.
[21] Rayner CR, Smith PF, Andes D, Andrews K, Derendorf H, Friberg LE, et al. Model-informed drug development for anti-infectives: state of the art and future. Clin Pharmacol Ther 2021;109:867–91. https://doi.org/10.1002/cpt.2198.
[22] Boisson M, Mimoz O, Hadzic M, Marchand S, Adier C, Couet W, et al. Pharmacokinetics of intravenous and nebulized gentamicin in critically ill patients. J Antimicrob Chemother 2018;73:2830–7. https://doi.org/10.1093/jac/dky239.
[23] Nguyen THT, Mouksassi MS, Holford N, Al-Huniti N, Freedman I, Hooker AC, et al. Model evaluation of continuous data pharmacometric models: metrics and graphics. CPT Pharmacomet Syst Pharmacol 2017;6:87–109. https://doi.org/10.1002/psp4.12161.
[24] Dosne AG, Bergstrand M, Harling K, Karlsson MO. Improving the estimation of parameter uncertainty distributions in nonlinear mixed effects models using sampling importance resampling. J Pharmacokinet Pharmacodyn 2016;43:583–96. https://doi.org/10.1007/s10928-016-9487-8.
[25] Karlsson MO, Holford NHG. A tutorial on visual predictive checks. Population Approach Group Europe. Available At: https://www.page-meeting.org/?abstract=1434. [Accessed 8 November 2021].
[26] R: a language and environment for statistical computing. Vienna, Austria. Available at: https://www.r-project.org/. [Accessed 8 November 2021].
[27] Barclay ML, Begg EJ, Chambers ST. Adaptive resistance following single doses of gentamicin in a dynamic in vitro model. Antimicrob Agents Chemother 1992;36:1951–7.
[28] Barclay ML, Begg EJ. Aminoglycoside adaptive resistance: importance for effective dosage regimens. Drugs 2001;61:713–21. https://doi.org/10.2165/00003495-200161060-00001.
[29] USCAST, The National Antimicrobial Susceptibility Testing Committee for the United States. Aminoglycoside in vitro susceptibility test interpretive criteria evaluations. Available at: https://app.box.com/s/1hxc8inf8u3rranwmk3efx48upvwt0ww. [Accessed 8 November 2021].
[30] EUCAST. European Committee on Antimicrobial Susceptibility Testing. Gentamicin: rationale for the clinical breakpoints, version 2.0 2020. https://www.eucast.org/fileadmin/src/media/PDFs/EUCAST_files/Rationale_documents/Gentamicin_rationale_1.2_0906.pdf. [Accessed 8 November 2021].
[31] Torres BGS, Helfer VE, Bernardes PM, Macedo AJ, Nielsen EI, Friberg LE, et al. Population pharmacokinetic modeling as a tool to characterize the decrease in ciprofloxacin free interstitial levels caused by Pseudomonas aeruginosa biofilm lung infection in Wistar rats. Antimicrob Agents Chemother 2017;61:e02553-16. https://doi.org/10.1128/AAC.02553-16.